SPECIAL SESSION

https://doi.org/10.1590/2317-4889202120210040

BJGEO Brazilian Journal of Geology

High-resolution stratigraphy of peritidal microbial carbonates from the Lagoa do Jacaré Formation, Bambuí Group, north of Minas Gerais state, Brazil

Samuel Amaral Moura[1]*, Alexandre Uhlein[2], Gabriel Jubé Uhlein[2], Márcio Vinicius Santana Dantas[1]

Abstract

High-resolution stratigraphic analysis was carried out on tidal microbial carbonates from the middle part of the Lagoa do Jacaré Formation from the Ediacaran-Cambrian Bambuí Group in the Ubaí area. In a 41 meter-thick section, sixteen lithofacies and three facies associations were interpreted as deposits of supratidal, intertidal, and subtidal settings. The tidal cycles are asymmetric and shallow upward, the high-resolution stratigraphic approach allowed inferences as to short-term and long-term fluctuations of sea level during deposition. The metric tidal ranges here described suggest strong tidal currents, which is incompatible with the giant enclosed sea model as an analog for Bambuí deposition, given that tidal ranges in suc seas are null or less than a few decimeters. Therefore, we suggest that the Ubaí carbonates were deposited in a semi-enclosed epicontinental sea subject to strong tidal forces when the formerly resticted Bambuí Basin reopened probably during deposition of the upper half of the Lagoa do Jacaré Formation, as suggested by previous isotopic data and now reinforced by our sedimentologic and stratigraphic field data.

KEYWORDS: tidal cycles; cyclostratigraphy; stacking patterns; restricted basin; Ediacaran.

INTRODUCTION

Microbialites are carbonate rocks defined by Burne and Moore (1987) as organosedimentary deposits formed from the interaction between benthic microbial communities and detrital or chemical sediments (Dupraz *et al.* 2009). Microbialites (or microbial mats as their non-lithified equivalent) have high chemical gradients, an abundance of phototrophic microorganisms, and stratification of the microbial populations into distinct layers (e.g., Van Gemerden 1993, Visscher and Stolz 2005, Konhauser *et al.* 2007). These carbonatic rocks have been present since the Archean (e.g., Schopf *et al.* 2007) and are common deposits in continental and marine environments until today (Myshrall *et al.* 2010, Vasconcelos and Bahniuk 2015, Yanez-Montalvo *et al.* 2020). They are commonly found in nearshore environments, often subjected to tidal currents and arranged broadly in zones parallel to the coastline. The zonation of microbial mats, stromatolites, and thrombolites has generally been related to frequency and intensity of inundation and desiccation within the littoral zone (e.g., Logan *et al.* 1974, Jahnert and Collins 2011).

The purpose of this paper is to analyze the stratigraphic record of tidal microbialites and associated carbonatic rocks of the Lagoa do Jacaré Formation in the Ubaí area, north of Minas Gerais, from a high-resolution systematic approach. The deposition of the Lagoa do Jacaré Formation (Bambuí Group, Brazil) either occurred in the last million years of the Ediacaran Period, near the Ediacaran — Cambrian boundary, a time with unprecedented and definitive changes in every superficial layer of the Earth (Canfield *et al.* 2007, Meert and Lieberman 2008, Gaucher *et al.* 2009, Erwin *et al.* 2011, Och and Shields-Zhou 2012, Na and Kiessling 2015, Zhu *et al.* 2017). These changes were related to the decreased number of microbialite record during the Ediacaran-Cambrian transition (e.g. Awramik 1971, Riding 2006). This particularity is noticed in different sedimentary basins (e.g. Li *et al.* 2021). It is also present in the Bambuí Basin where there was a vast number of occurrences and of microbialites morphotypes at the base when compared to other younger carbonate formations of Bambuí Group (Fairchild and Sanchez 2015).

In the last few years, a rise in the number of studies involving the Lagoa do Jacaré Formation occurred (Uhlein *et al.* 2019, Cui *et al.* 2020, Caetano-Filho *et al.* 2021, Freitas *et al.* 2021), mainly due to the growing attention in highly positive $\delta^{13}C$ carbonates in Ediacaran successions worldwide (Kaufman *et al.* 2009, Moynihan *et al.* 2019). This unit registers a highly

[1]Programa de Pós-Graduação em Geologia, Instituto de Geociências, Universidade Federal de Minas Gerais – Belo Horizonte (MG), Brazil. E-mails: amaralms.samuel@gmail.com, auhlein@gmail.com

[2]Instituto de Geociências, Universidade Federal de Minas Gerais – Belo Horizonte (MG), Brazil. E-mails: guhlein@gmail.com, marcio_ufs08@hotmail.com

*Corresponding author.

positive $\delta^{13}C_{carb}$ excursion with values between +8‰ to +16‰, which is associated with the Middle Bambuí positive isotope Excursion (MIBE; Uhlein *et al.* 2019, Cui *et al.* 2020). The MIBE event is possibly related to the restriction of the basin water caused by the advance and uplifting of marginal Neoproterozoic-early Paleozoic orogens, as suggested by isotopic and elemental data, U-Pb ages and paleotectonic reconstructions (Reis *et al.* 2017, Uhlein *et al.* 2019, Cui *et al.* 2020, Caetano-Filho *et al.* 2021, Caxito *et al.* 2021). Despite the intensive studies on the Bambuí Group, the origins of the MIBE and a putative reopening of the basin to global oceans remain unanswered.

Earlier studies on the study area were made on a regional scale, therefore, the data presented in this paper is novel in terms of high-resolution stratigraphy and cyclicity definition of microbial carbonates and associated lithofacies from the Lagoa do Jacaré Formation. Therefore, we bring a new point of view on the sequence stratigraphic aspects and paleoenvironmental evolution of tidal microbialites as well as the Lagoa do Jacaré Formation.

GEOLOGICAL SETTING

The Bambuí Group records an extensive foreland basin, initiated in response to the diachronic lithospheric overburden experienced by the São Francisco plate caused by the uplift of the Brasília (west) and Araçuaí (east) fold belts, during the Ediacaran and Cambrian Periods. The basin covers hundreds of thousands of square kilometers in the states of Minas Gerais, Bahia, Goiás, and Tocantins, in east-central Brazil (Alkmim and Martins-Neto 2001, Martins-Neto 2009, Sial *et al.* 2009, Uhlein 2017). The stratigraphic organization in a foreland basin is remarkably different according to the distance from the fold belts, so the Bambuí Group may be divided roughly into three sectors: west, central, and east (Uhlein *et al.* 2017).

The study area is located on the Januária high-land basement in the east sector, which comprises a mixed carbonate-siliciclastic sedimentary succession deposited under conditions of low subsidence rates and strong eustatic control (Castro and Dardenne 2000, Martins-Neto and Alkmim 2001, Martins and Lemos 2007, Reis *et al.* 2016, Uhlein *et al.* 2019). In this area, the Bambuí Group, is composed from the bottom to the top of the Sete Lagoas Formation (limestone and dolomite), Serra de Santa Helena Formation, (siltstone and carbonate), Lagoa de Jacaré Formation, (reworked carbonate rocks and some microbialite), Serra da Saudade Formation (siltstone, sandstone, and carbonate of the Jaíba Member), and Três Marias Formation, (arkose and conglomerate) (Uhlein *et al.* 2019). It is important to highlight that the basement structures of the Bambuí basin performed an important control during the deposition of the homonymous group. These are named Januária high-land basement, Sete Lagoas high-land basement, and Pirapora aulacogen, which were identified based on geophysical, field, and borehole data. (Magalhães 1989, Alkmim and Martins-Neto 2001, Zalán and Romeiro-Silva 2007, Hercos *et al.* 2008, Reis *et al.* 2017; Fig. 1).

U-Pb detrital zircons and chemostratigraphic data suggest that the deposition of the Bambuí Group occurred in the Ediacaran (Pimentel *et al.* 2011, Caxito *et al.* 2012, Paula-Santos *et al.* 2015). Moreover, the occurrence of biomineralized

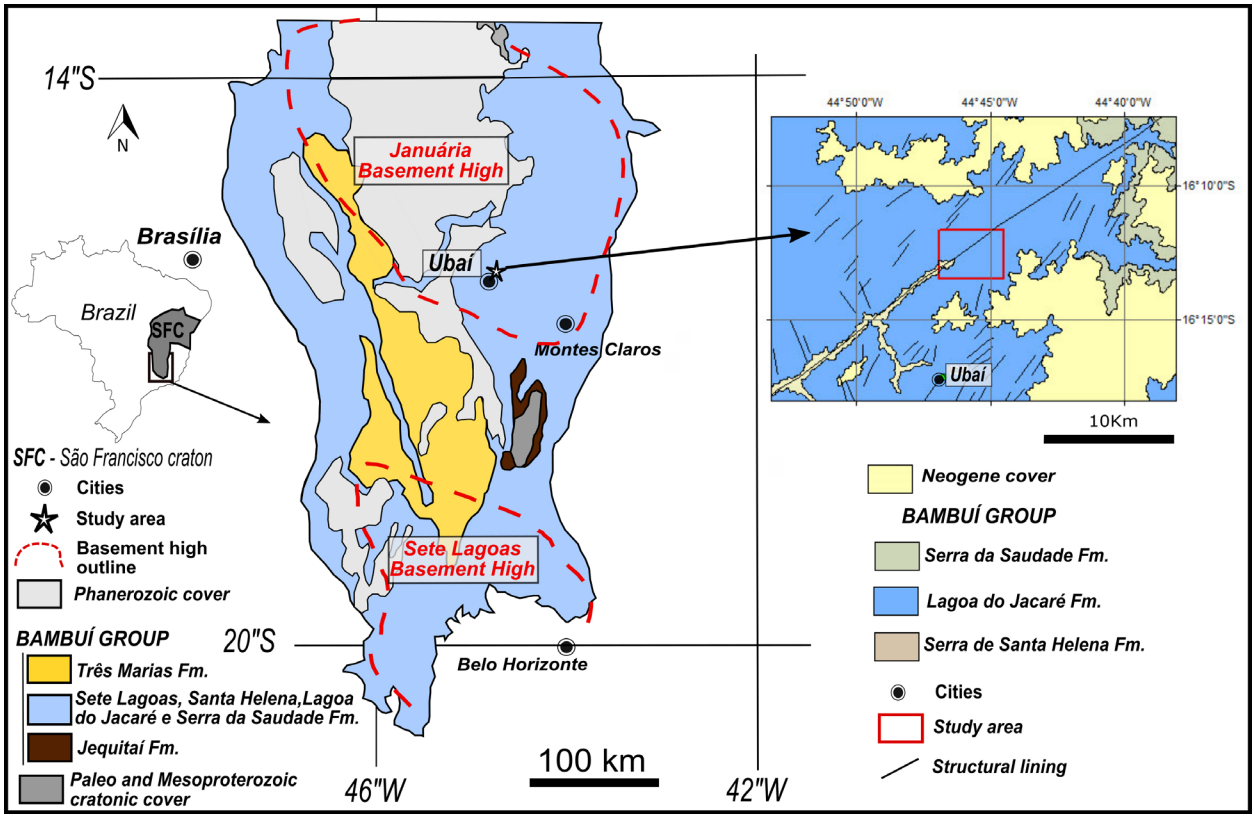

Source: geologic maps based on Misi (2001), Heineck *et al.* (2003), Uhlein *et al.* (2014), and Reis *et al.* (2017).
Figure 1. Geological setting and location of the study area in the Ubaí area, north of Minas Gerais state.

metazoans most likely associated with *Cloudina sp*. in the middle of the Sete Lagoas Formation, strongly suggests a deposition at the end of the Ediacaran Period (Warren *et al*. 2014, Uhlein *et al*. 2019). More recently, zircon grains from a tuff layer in the Serra da Saudade Formation (Moreira *et al*. 2020) and *Treptichnus pedum* occurrences in the Três Marias Formation (Sanchez *et al*. 2021) extended the depositional history of the upper Bambuí Group into the Cambrian Period.

The Lagoa do Jacaré Formation presumably formed near the transition interval between the Ediacaran and Cambrian periods. It is described as reworked black carbonate, from grainstone to mudstone and rare shale, often presenting well-preserved ooids, that were deposited on inner to outer shelf environment (e.g., Dardenne 1978, Misi *et al*. 2007, Freitas *et al*. 2021). The Lagoa do Jacaré Formation is mainly famous for its carbonatic rocks with positive values of $\delta^{13}C$, as high as +16‰, regardless of the studied section. This interval of highly positive carbon isotope values was named MIBE (Middle Bambuí Excursion) and extends for around 350 m along the Bambuí Group (Uhlein *et al*. 2019). Recently, Cui *et al*. (2020) and Caetano-Filho *et al*. (2021) explored the MIBE using a diverse set of geochemical tools and, among other hypotheses, they interpreted a methanogenic and highly restricted basin during the deposition of the Lagoa do Jacaré Formation. There are few microbialite occurrences in the Lagoa do Jacaré Formation (Ribeiro *et al*. 2008, Iglesias and Uhlein 2009, Signorelli 2009, Kuchenbecker and Pedrosa-Soares 2010, Atman 2011, Fragoso *et al*. 2011). The morphotypes suggest a relation with a small barrier reef and a wave-protected peritidal environment (Santos *et al*. 2018) formed during the end of a regional regression trend (Uhlein *et al*. 2019). On the Januária high basement, the Bambuí Group may be subdivided into five transgressive-regressive 2nd-order sequences. The second-order maximum regression surface is positioned in the middle of the Lagoa do Jacaré Formation, where microbialites and other tidal like lithofacies dominate and overlaid, there is the beginning of a new transgression trend (Uhlein *et al*. 2019).

MATERIALS AND METHODS

The sedimentologic and stratigraphic data presented in this paper are composed of 27 outcrops located in an area close to the Ubaí town, north of Minas Gerais, Brazil (Fig. 1). The dimensions of the study area are 3 km in the east-west direction and 4,5 km in the north-south direction (Fig. 2). The stratigraphic

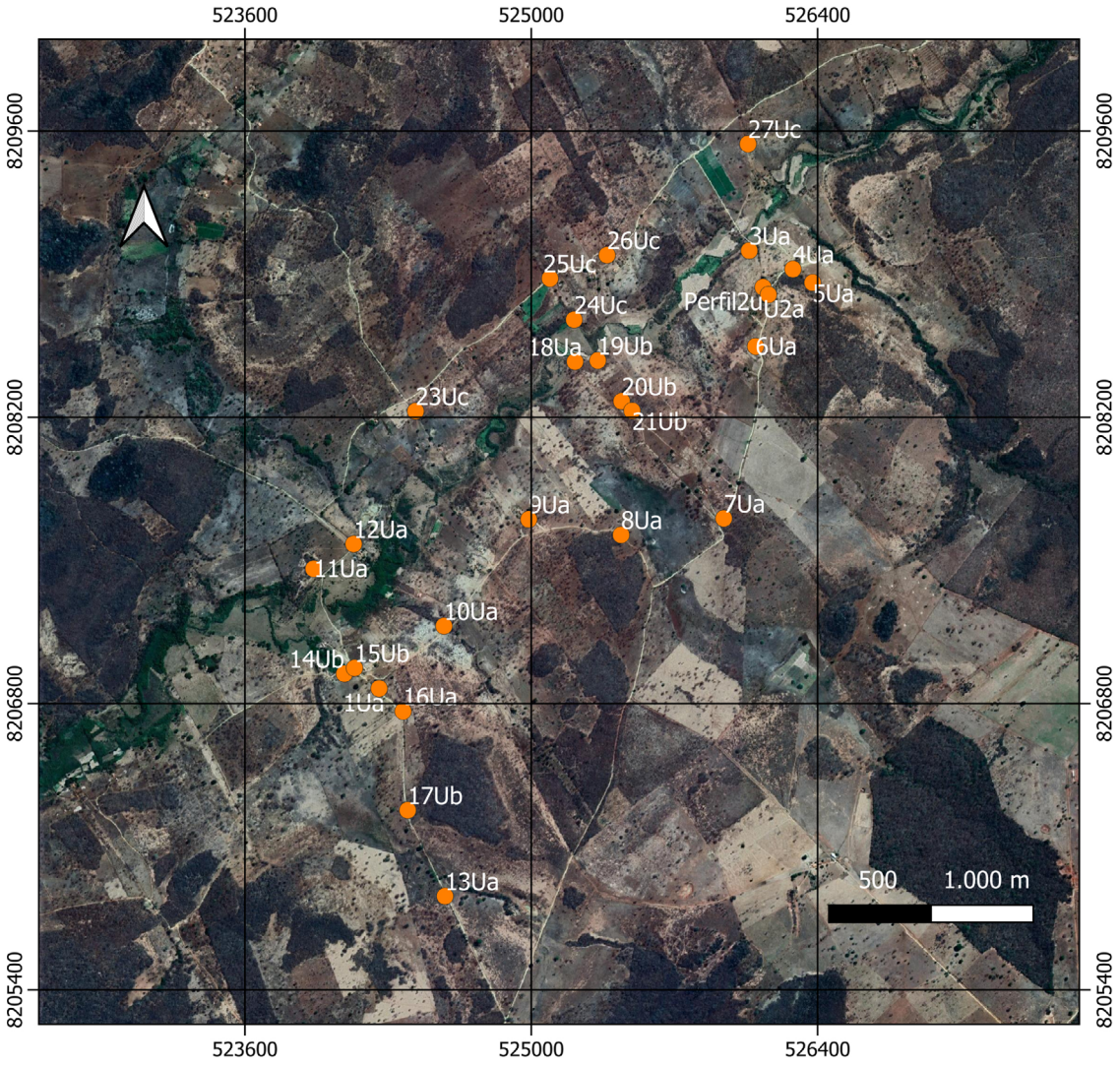

Figure 2. The study area and the location of the 27 outcrops described.

survey scale is 1:20. Due to the vertical continuity, only 25 vertical profiles were selected to make up the 41 m-thick interval of the Lagoa do Jacaré Formation. Lithofacies were classified according to the classic works of Dunham (1962), Folk (1962), Embry and Klovan (1971), Demicco and Hardie (1994); and Riding (2000, 2011). The characteristics of the carbonate microfabric observed under the microscope were important for the classification of facies. The facies codes are similar to the codes proposed by Miall (1977) for river systems, in which the texture of the lithofacies is presented in capital letters and small letters designate the main structure present or an important feature.

According to Embry (1993, 1995) the definition of the transgressive and regressive (T-R) cycles allow us to identify cycles with different orders in the study's sedimentary record. The regional Bambuí stratigraphic context (e.g., Uhlein *et al.* 2019) and classic works in high-resolution stratigraphy (e.g., Read and Goldhammer 1988, Goldhammer *et al.* 1990, Osleger and Read 1991) were used for sequence stratigraphic interpretations and basin correlations. The interpretation of the stratigraphic cycle was based on general concepts pointed out by Catuneanu (2019), but specific works on sequence stratigraphy of phanerozoic tidal plains (e.g., Spence and Tucker 2007) allowed an assertive interpretation of the sequence's orders. Pratt (2010) points out that, in general, the thickness of the tide cycle is proportional to sea-level variations and this was crucial to understand the limits of the higher-order cycles as well as interpreting short and long-term sea level changes.

PERITIDAL RECORD OF THE LAGOA DO JACARÉ FORMATION IN UBAÍ AREA

Lithofacies and depositional processes

Proceeding the detailed description of the outcrops, sixteen lithofacies were identified (Tab. 1; Figs. 3 and 4) and classified into five textural groups: organosedimentary carbonates, mud carbonates, heterolithic carbonates, sandy carbonates, and conglomeratic carbonates. These groups do not correspond to the lithofacies association and they exist just to simplify the description process.

Four lithofacies constitute the organosedimentary carbonate group: microbial laminite (ML; Fig. 3A), microbial laminite with boudin-like structure (MLb; Fig. 3B), mudstone interlayered with microbial laminite (MML), and thrombolite (TB; Fig. 3C). The genesis of this group of carbonates (microbialites) results mainly from the process of organomineralization (microbially induced and influenced mineralization) (Dupraz *et al.* 2009). It is related to the metabolic activity of the synergistic associations of a microbial mat, and the complex interactions between these biofilms and their surrounding environment can result in the production of microbialites lithofacies (Riding 2011, Bosak *et al.* 2013, Vasconcelos *et al.* 2014).

The ML and MLb facies are characterized by their intercalated light and dark layers. The lightest colored layers are mainly made up of mudstone and rarely wackestone or grainstone, with peloids as the main component. The dark layers have a relatively larger amount of clay minerals, micas, quartz, and carbonaceous matter. Framboidal pyrite and calcite-filled birds-eye structure (Figs. 5A and 5B) are common features of the ML and MLb facies, that are most likely the result of metabolic activities of microbial mats, responsible for organic matter remineralization, pyrite formation, and $CaCO_3$ precipitation, among many other processes, (e.g., Visscher and Stolz 2005, Konhauser *et al.* 2007).

The MLb lithofacies stands out due to the sedimentary boudinage structure, the result of differential compaction of patchy carbonate deposits. These deposits form irregular, closely spaced structures caused by a disruption of layers by stretching. Therefore, we can observe microfractures, microfaults, domino-like features, and lateral discontinuities (Fig. 5A) on thin sections. It is important to highlight that they are often associated with tepee and likely evaporite pseudomorphs (Fig. 6). Therefore, these microfabric aspects could also be related to salt precipitation.

The mud carbonates group consists of massive mudstone (MUD), mudstone with shrinkage cracks (MUDdc), and mudstone with syneresis cracks (MUDsc). The mud carbonates contain a small portion of allochems, which can reach up to 5%, but their distribution is not restricted to preferential levels. Peloids have diameters ranging from 0.03 to 0.1 mm, and the frequent presence of framboidal pyrite and fenestrae filled with sparry calcite shows a plausible organosedimentary influence on the deposition of mudstones.

The group of heterolytic carbonates consists of carbonates with lenticular bedding (Hlb; Fig. 4B), as well as low angle cross-lamination (Hcl; Fig. 4D). The lenticular bedding structure is formed by the intercalation of peloidal (diameters from 0.03 to 0.1 mm) sand carbonate interspersed with mudstone. The low-angle cross-lamination structure of some heterolytic carbonates is formed by the alternation between layers predominantly composed of calcitic mud and others with idiotopic mosaic of euhedral dolomite rhombs. The dolomitized levels were fundamental for demarking a primary sedimentary structure. However, it is not possible to identify the primary attributes of that level, so it is unknown whether the dolomitized levels would be wackestone, packstone, or grainstone and which allochems compose these levels.

Five facies constitute the sandy carbonate group: massive packstone (PCK), packstone with horizontal lamination (PCKhl; Fig. 4A), packstone with low-angle cross-lamination (PCKcl; Fig. 4C), packstone with current ripple (PCKcr), and packstone with swaley cross-stratification (PCKscs; Fig. 4F). The sandy carbonates contain 50 to 60% of allochems composed mainly of peloids with diameters ranging from 0.06 to 0.2 mm dispersed in a locally micritic recrystallized matrix. In bedded packstones intercalations of packstone and wackestone layers often occur (Fig. 5C). The wackestone layers are characterized by 15 to 25% of peloids with diameters ranging from 0.3 to 0.13 mm, dispersed in a micrite matrix.

The group of conglomeratic carbonates is composed of floatstone (FLT; Fig. 4E) and rudstone (RUD), all showing a lenticular geometry. On the thin sections, these lithofacies are mainly composed of fine peloid grains. The coarse sand to

Table 1. Lithofacies: Macroscopic characterization and Interpretation.

Facies Code	Lithofacies	Sedimentary structure	Petrographic Characterization	Depositional processes
ML	Microbial Laminite	Laminated or thinly bedded	Mudstone and microbial mat intercalation	organomineralization, trapping and binding
MLb	Microbial Laminite with boudin-like structure	Laminated or thinly bedded with sedimentary boudinage	Mudstone and microbial mat intercalation with boudin-like structure some layers	organomineralization, trapping binding, desiccation, and differential compaction of patchy deposits
MML	Mudstone interlayered with Microbial laminite	Laminated with little lateral continuity	Thick and discontinuos laminated microbial mat in mudstone	organomineralization, trapping and binding
MUD	Mudstone	_	Massive gray mudstone	organomineralization and carbonate mud precipitation
TB	Thrombolite	Clotted texture	Microbialite with clotted texture	organomineralization, trapping and binding
MUDdc	Mudstone with desiccation crack	Shrinkage crack	Mudstone with shrinkage cracks that is filled with carbonate sand or microbial mat	organomineralization, carbonate mud precipitation and desiccation
MUDsc	Mudstone with syneresis crack	Syneresis crack	Mudstone with incomplete polygonal pattern and with either bird's foot or spindle shape	Salinity changes and osmotic effects
HClb	Heterolithic carbonate with lenticular bedding	Lenticular bedding	Light gray mudstone with dark fine gray carbonate sand lenses	Fluctuations in sediment supply or intensity of current activity
HCcl	Heterolithic carbonate with cross-lamination	Low-angle cross-lamination	Heterolytic mudstone and dolomite preserving the cross-laminations	subaqueous currents in lower flow regime in waning flood deposits
PCK	Massive packstone	_	Dark gray carbonate composed of fine-grained sand	Pseudoplastic debris flow
PCKcl	Packstone with cross-lamination	Low angle Cross-lamination	Dark gray carbonate sand with interleaving between very fine and fine grains	subaqueous currents in lower flow regime
PCKhl	Packstone with horizontal lamination	Horizontal lamination	Dark gray carbonate with interleaving between fine- and medium-grained sand layers	subaqueous currents in lower flow regime
PCKcr	Packstone with current ripple	Linguoid current ripple	Dark gray carbonate sand composed of very fine and fine grains	subaqueous currents in lower flow regime
PCKscs	Packstone with swaley cross-stratification	Swaley cross-stratification	Dark gray carbonate sand composed of very fine and fine grains	Result of storm waves
FLT	Floatstone	Massive and lenticular geometry	Matrix supported, massive carbonate gravel. The matrix is composed of fine gravel and the coarse fraction is composed by rounded granules and pebbles. Although some may be angular	Pseudoplastic debris flow (low strenght, viscous)
RUD	Rudstone	Massive and lenticular geometry	Clast-supported carbonate gravel. The matrix is composed of fine gravel and the coarse fraction is composed mainly by rounded granules and pebbles.	Pseudoplastic debris flow (inertial bedload, turbulent flow)

pebble-sized grains and clasts are compound by poorly preserved ooids (Fig. 5F), intraclasts of mudstone, packstone (Fig. 5D), and microbial laminite (Fig. 5E). The intergranular part is filled mainly by micrite matrix and in some portions, by sparry cement.

Lithofacies successions

The Lagoa do Jacaré Formation deposits in the Ubaí area, are composed of vertically-stacked microbial laminite, mud carbonate, packstone, heterotithic carbonate, and carbonatic conglomerate. All of these could occur in different proportions through the succession, and may show different facies relationships between them. As a result, an array of different possible facies stacking patterns can be observed, which have been analyzed thoroughly in the 25 detailed columnar sections measured in the best exposed stratigraphic interval of the study area (Fig. 7).

The peritidal carbonate environment of the Lagoa do Jacaré Formation in the Ubaí area was a mud flat with spread microbial mats. Tidal channels and related deposits composed of packstone, floatstone and rudstone occur across this environment. These related deposits are formed when a stream breaks its natural or artificial levees and deposit sediments in this mud tidal plain. Therefore, this record can be divided

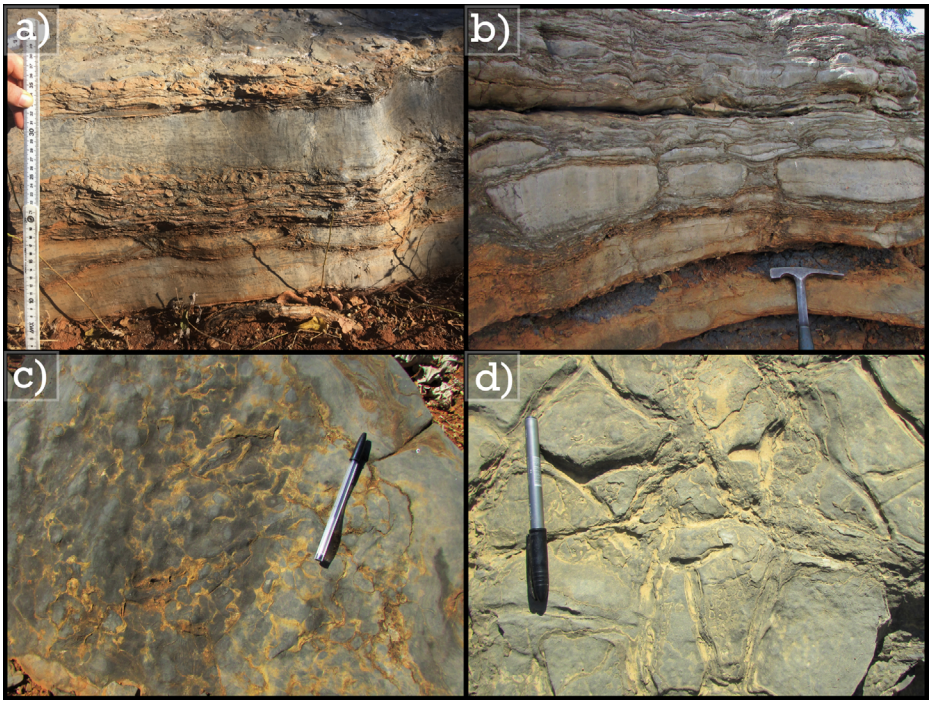

Figure 3. Lithofacies of the Lagoa do Jacaré Formation; (A) microbial laminite (ML); (B) microbial laminite with boudin-like structure (MLb); (C) thrombolite (TB); (D) mudstone with desiccation crack (MUDdc);

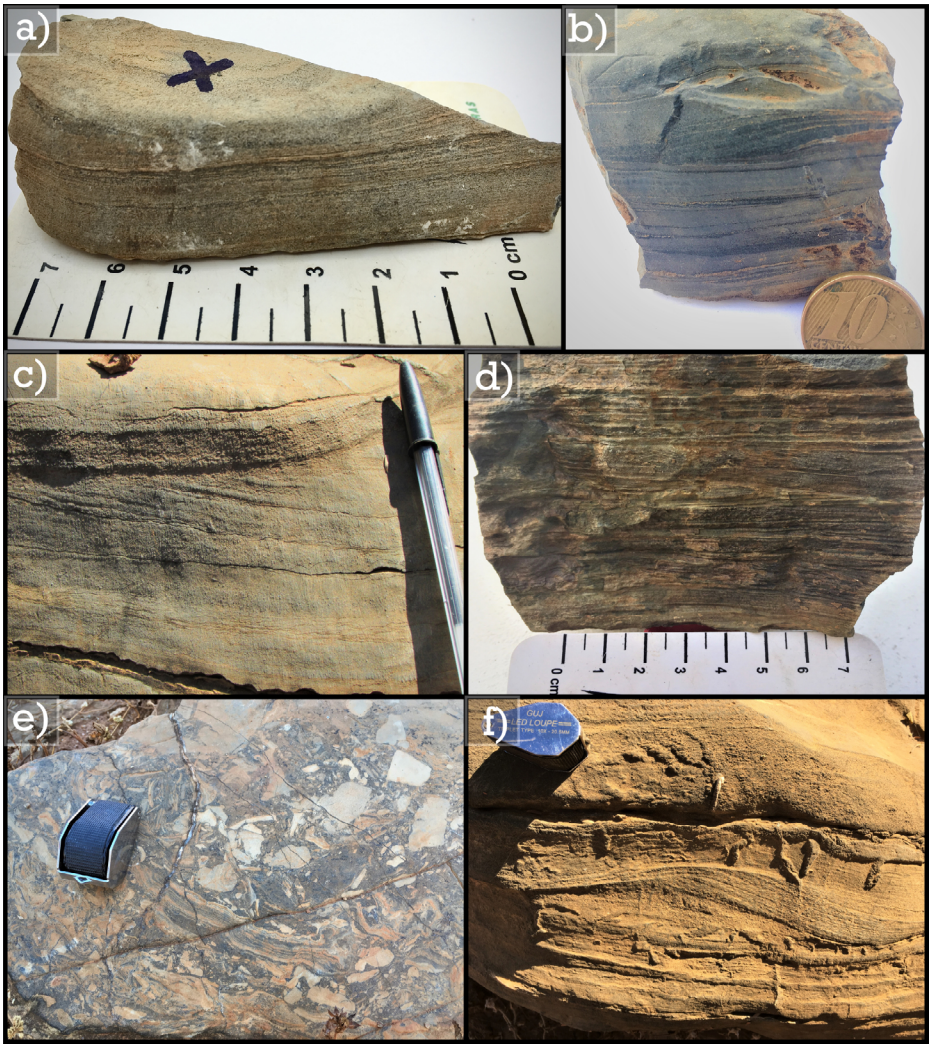

Figure 4. Lithofacies of the Lagoa do Jacaré Formation; (A) packstone with horizontal lamination (PCKhl); (B) heterolitic carbonate with lenticular bedding (Hlb); (C) packstone with low angle cross-lamination (PCKcl); (D) heterolithic carbonate with very low angle cross-lamination (Hcl); (E) floatstone with angular granules and pebbles (FLT); (F) packstone with swaley cross-stratification (PCKscs) below syneresis cracks.

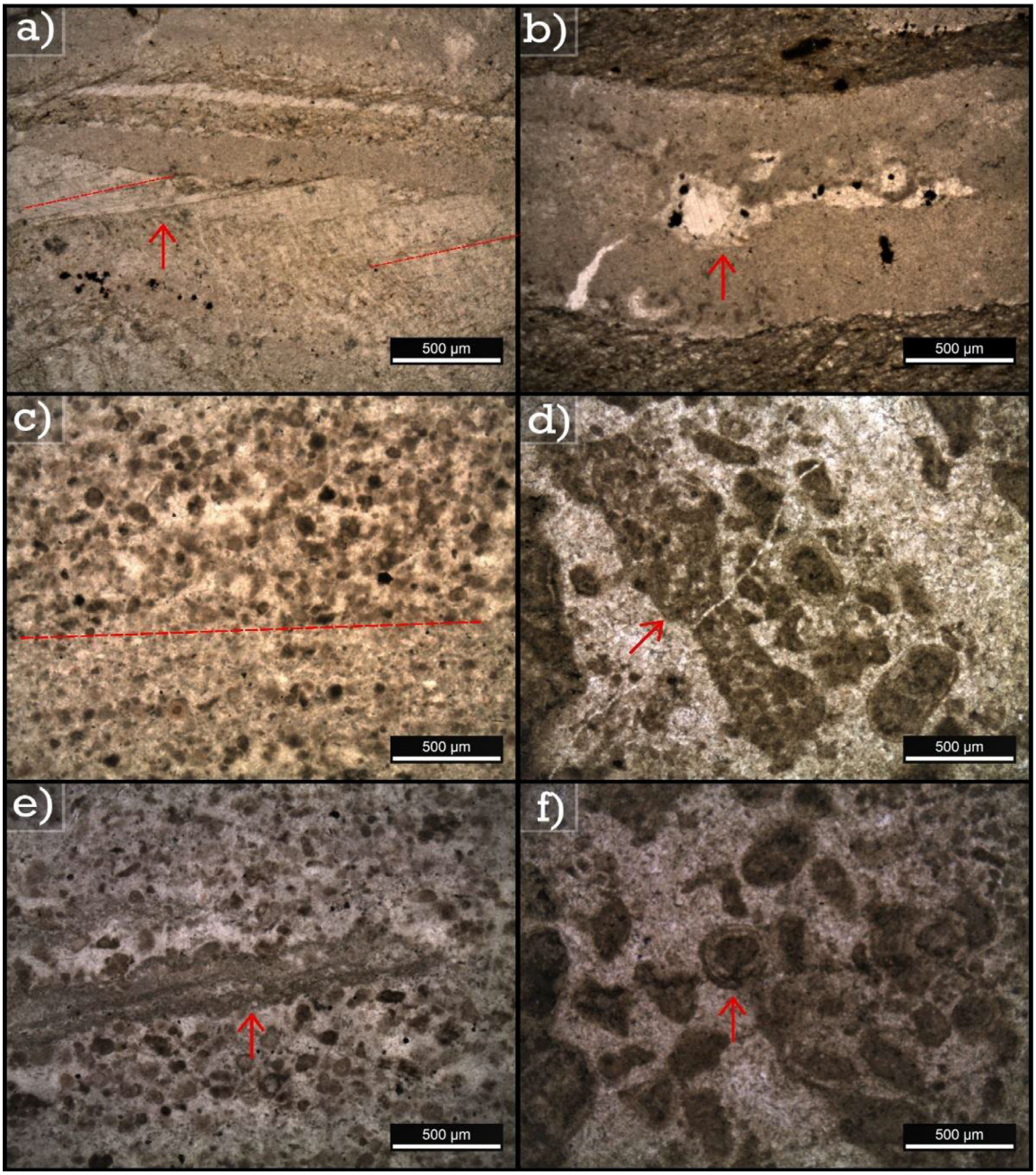

Figure 5. Carbonate microfacies of Lagoa do Jacaré Formation. (A) Domino microstructure probable associated with salt precipitation or the result of differential compaction of patchy deposits of carbonate. (Lithofacies MLb); (B) Fenestras or birds-eye filled by two generations of sparry calcite and framboidal pyrite in a mudstone interlayered by two organic-rich layers (Lithofacies LM and LMb); (C) The sedimentary structure of packstones formed by the intercalation of wackestone (in the lower part) layer and packstone (in the upper part) layer (PCKcs and PCKhl); (D) The framework of FLT lithofacies is filled by sparry cement where a packstone intraclast and some peloids are seen (E) Microbial laminite intraclast immersed in peloids. (PCK and FLT) (F) Poorly preserved ooid (RUD and FLT).

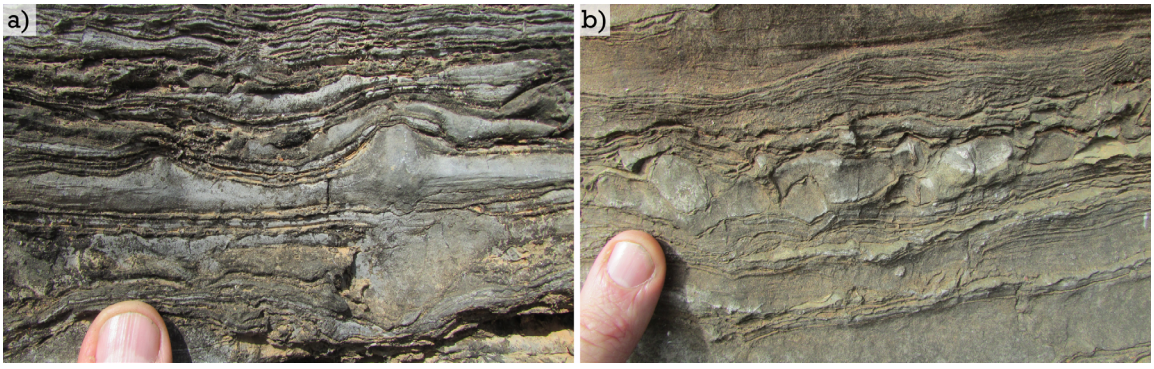

Figure 6. MLb facies. (A) Occurrence of tepees in the microbial laminites; (B) large calcite crystals probable after evaporite minerals adjoined by microbial laminite below and above.

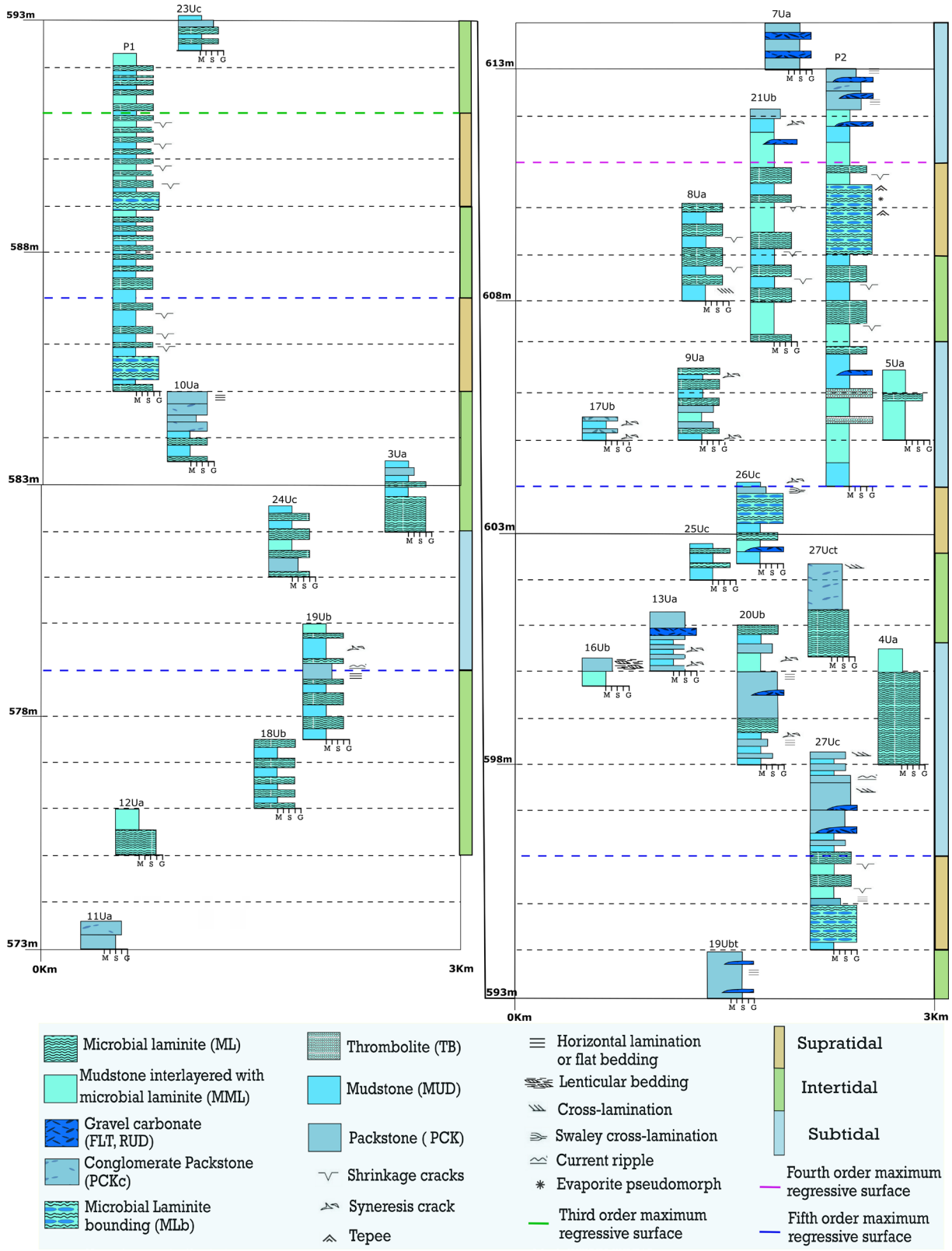

Figure 7. The stratigraphic panel was made with data collected in the field. It shows the east-west distribution of the stratigraphic survey. On the left, the sections are between 573 to 593 meters (the bottom record of the studied interval). On the right, they are between 593 to 614 meters (the top record of the Lagoa do Jacaré Formation in the Ubaí area). The colored vertical bar on the right of the panels shows the lithofacies successions interpretation related to supratidal, intertidal, and subtidal zones.

in subtidal, where the sedimentary processes are subaqueous; intertidal, where subaqueous and subaerial processes occur; and supratidal, where subaerial processes occur almost exclusively (Tucker and Wright 1990). Although this subdivision is definitive in terms of sediment-water interaction, a challenge to be surpassed is that the same facies can occur in different tidal zones (Fig. 8). After all, there are sedimentary processes that can occur in more than one of these sub-environments (Jimenez de Cisneros and Vera 1993, Haas *et al.* 2007, Quijada *et al.* 2020). To aid this type of study, Pratt (2010) developed

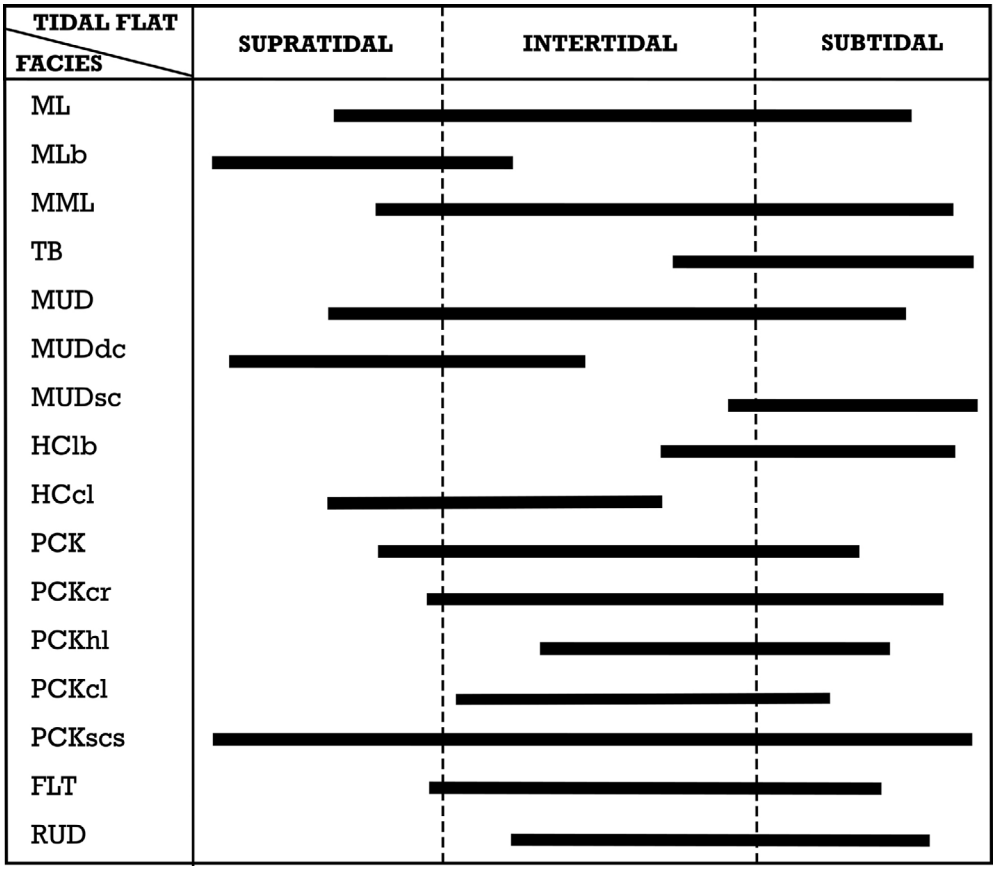

Figure 8. Facies determined in the field and their occurrence in the different settings of a peritidal environment.

a table-guide to identify sedimentary features and their distribution in the three zones of the aforementioned tidal environment. Based on this guide, it is possible to create a similar table using the lithofacies presented in the current research (Fig. 8).

There are some diagnostic facies associations that can be used to properly identify the tidal settings. The occurrence of MLb with MUDdc indicates the supratidal zone, since these structures form through desiccation on exposure (subaerial process). The co-occurrence of TB, Hlb, and MUDsc are indicative of subtidal zones. The MUDsc form through sediments dewatering, subaqueous, often resulting from salinity changes. The Hlb form through variations of sediment supply or intensity of currents in subaqueous environments. The natural duality presented in the intertidal zone (i.e., subaerial and subaqueous processes) makes this zone of arduous identification (Tucker 2003), thus the use of a proper stratigraphic panel from detailed stratigraphic descriptions is crucial.

The vertical and lateral relationships of the Lagoa do Jacaré lithofacies (Fig. 7) helped to define the intervals of each facies association and its repetition through the studied section. The repetitive vertical patterns are cyclicity expressions that respond to allogenetic mechanisms. On the other hand, the patchy lateral facies distribution suggests some variation that is most likely linked with autogenic mechanisms related to hydraulic factors. These variations occur according to the environment's divisions, and thus the facies arrangement produces a vertical succession of facies that can be subdivided into shallowing-upward, decimeter to meter-thick cycles (Pratt 2010, Yang *et al.* 2014, Zhang *et al.* 2015). Identifying the boundary of these shallowing upward cycles was not an easy task, since there were a lot of surfaces in the supratidal zone and they are related to subaerial exposure. Therefore, in order to evaluate the allogenic meaning of these surfaces, we need to analyze their lateral continuity and the overlap by facies related to subaqueous processes.

DISCUSSION

Analysis of stratigraphic ciclicity

The stacking pattern of the Lagoa do Jacaré Formation in the Ubaí area indicates that the sediments accumulated during a marine transgression punctuate higher-order fluctuation in relative sea-level (Fig. 9). The minor fluctuations produced m-scale cycles is interpreted as peritidal carbonatic cycles in shallow, low angle, carbonate ramps (James 1984, Jimenez de Cisneros and Vera 1993, Pratt 2010).

The peritidal cycles reflected allogenic mechanisms that led to the episodic creation of accommodation filled by regional progradation, retrogradation or aggradation. Spencer and Tucker (2007) show that phanerozoic tidal cycles are of the fourth or fifth order. All over the geologic time, the overall characteristics of these cycles are similar, as we can see in the Mesoproterozoic (Wright and Burchette 1996); Ediacaran (Drummond *et al.* 2015, Caird *et al.* 2017); Late Cambrian (Osleger and Read 1991); Ordovician (Hersi and Dix 1999); Early Jurassic (Bosence *et al.* 2000); and Middle Triassic (Peterhänsel and Egenhoff 2008). Catuneanu (2019)

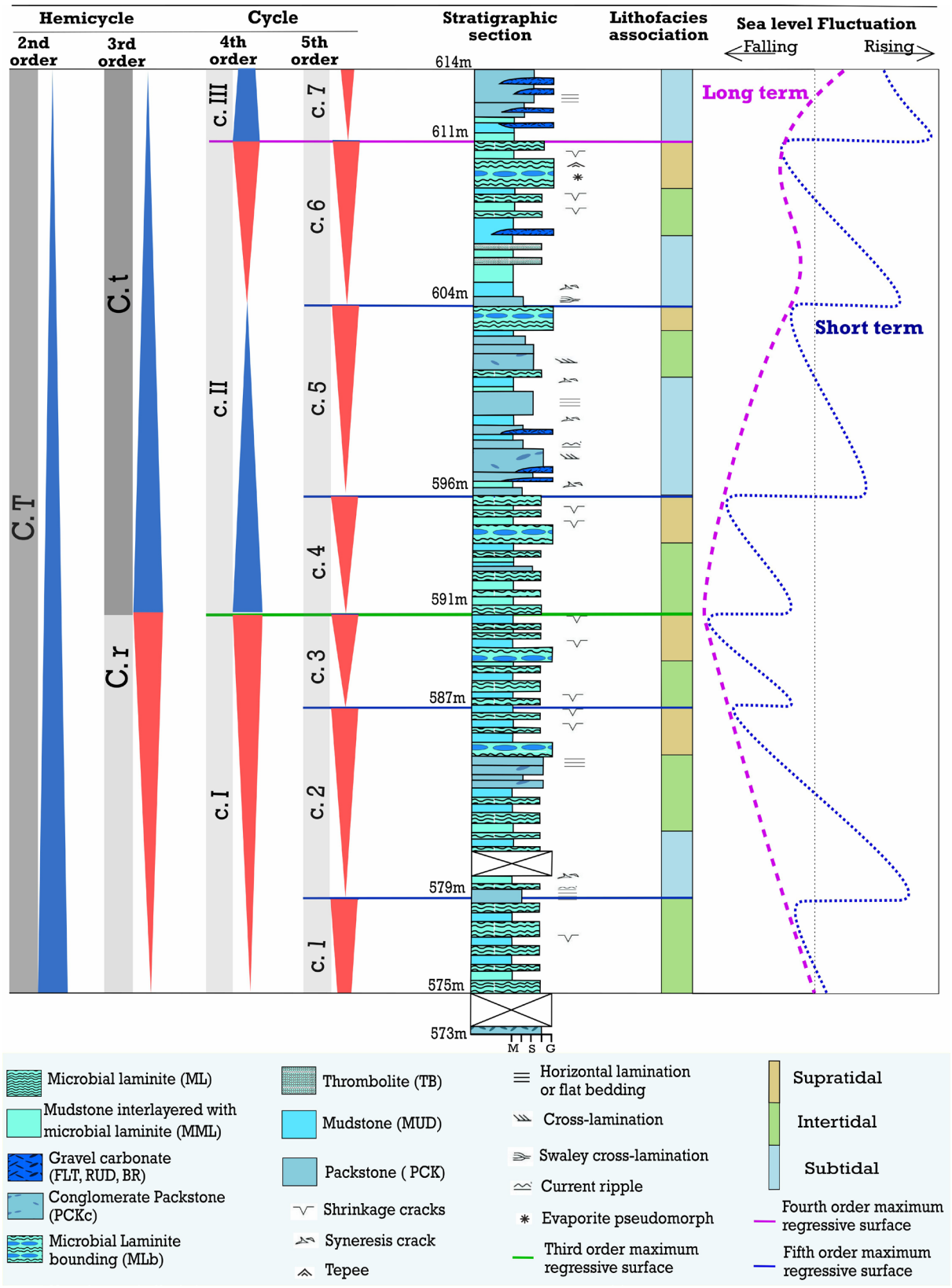

Figure 9. Stratigraphic section of the Lagoa do Jacaré Formation in Ubaí area. Facies associations, stratigraphic cycles, and fluctuations in sea level during its deposition.

proposes a solution to determine cycle orders without fossil content or other evidence indicating a more precise depositional age. The thickness of the sedimentary package can be related with the order of the cycle (Spencer and Tucker 2007). Therefore, it was possible to identify one second order hemicycle, two third order hemicycles, three fourth order cycles, and seven fifth order or peritidal cycles in the Lagoa do Jacaré Formation (Fig. 7).

Fifth order: asymmetrical tidal cycle

From a detailed facies analysis and defining tidal zones for each facies association, we identified seven shallowing-upward

tidal cycles. A theoretical and ideal tidal cycle (Fig. 10) in higher sea level fluctuation (c.Xhf) begins with conglomeratic and sandy carbonates interspersed by MUDsc, Hlb, ML, MML, and TB from the subtidal zone. Above this cycle, a shift is observed as more frequent beds of microbialite, mudstone and some subaerial exposure surfaces appear, while conglomeratic and sandy carbonate become less frequent. This shift is interpreted as a shallowing trend from sandy subtidal to muddy intertidal deposits. Finally, the theoretical tidal cycle culminates in a progressive and significant increase in the abundance of microbialite beds, mudstones and subaerial surfaces deposited in a supratidal zone (lithofacies MUD, MUDdc, MML, ML, MLb and some thin sandy bodies). The other idealized tidal cycle formed during lower sea level fluctuation (c.Xlf) is similar to c.Xhf with the exception of not recording the subtidal zone and its lithofacies associations. The largest content of organosedimentary lithofacies could be related to less reworking of these lithofacies and the most suitable conditions for the action of organo-sedimentary processes.

The fifth order cycles identified in this work show that the supratidal lithofacies association from a previous cycle often abruptly gives place to the subtidal zone of the following cycle (and no facies changes clearly demonstrate a progressive drowning) (Fig. 9) Therefore, the transgressive events were considered as non-recorded due to either fast reworking or non-deposition. Thus, we interpret the tidal cycles as asymmetric. The thicknesses of each fifth order cycle were used to estimate the sea-level fluctuations, that could theoretically yield an approximate measure of the tidal range when the eustatic level suffers only small changes (Masse *et al.* 2003, Pratt 2010). Thus, even without the transgressive record, the short-term sea-level fluctuations can be inferred (Fig. 9).

Each fifth-order tidal cycle in Fig. 9 is named with a lowercase "c" added to a number from 1 to 7. The seven identified shallowing upward tidal cycles have thicknesses ranging from 8 to 4 meters and as mentioned, due to the constant stacking of regressive intervals without intermediate transgressive trend, the tidal cycles are bounded between each other by amalgamated maximum regressive and maximum flooding surfaces. To simplify, we chose to designate these boundaries as regressive surfaces.

Fourth order T-R cycles

There are three fourth-order cycles. To name and identify each fourth-order T-R cycle, we use the lowercase "c" and a roman number from I to III (Fig. 9). The fourth-order cycles respond to longer-term fluctuations in sealevel and must be analyzed from a critical evaluation of the fifth-order tidal cycles. The thinning of the c1, c2, and c3 tidal cycles, the clear increase in the number of microbial laminite beds, and subaerial exposure surfaces toward the c2 and mainly the c3 cycles, are likely the result of a normal regression and progradation, which reduces the accommodation and proportionally increases the occurrence of facies related to inter and supratidal zones. From the upper c3 to the upper c5, the tidal cycles are arranged in a thickening-upward profile corresponding to a fourth-order transgression. The fact that c5 records the thickest tidal cycle and with a thick subtidal zone that was absent in c4 and c3 is noteworthy. The termination of the c5 is also marked by the absence of once common mud cracks and the low number of microbialite beds, suggesting an end to the tidal cycle in a slightly deeper environment than the previous ones. The consequence is the coincidence of a fourth-order maximum flooding surface (end of c.II) with the culmination of the

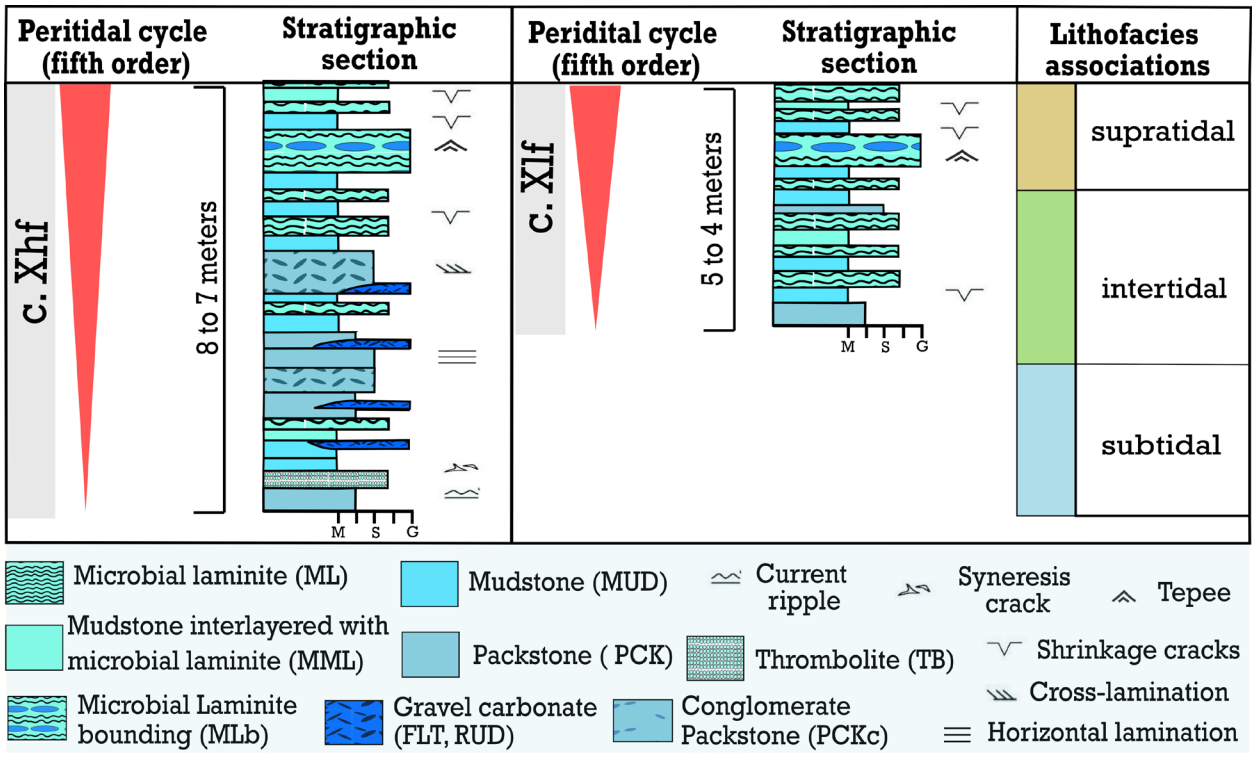

c.X: an idealized tidal cycle; C.Xhf: idealized cycle in higher sea level fluctuation; c.Xlf: idealized cycle in lower sea level fluctuation.

Figure 10. Idealized tidal cycles based on the lithofacies identified in the field and their distribution in the different sub-environments.

c5 tidal cycle. The tidal range (i.e., cycle thickness) from c5 to c6 decreases, and the upper c6 is marked by thick beds of MLb, other microbial laminites, a high number of beds with mud cracks, and evaporite pseudomorphs. Thus, a fourth-order regressive cycle is coincident with the fifth-order tidal cycle of c6. The c7 is an incomplete cycle, but the thicker subtidal zone and the greater occurrence of conglomeratic carbonates and packstones suggests that a new transgression initiates after the last fourth-order regression. Therefore, c1, c2, and c3 cycles were deposited during a higher-order regression (c.I), while c4, c5, and c6 record a complete transgressive-regressive fourth-order sequence (c.II). The c.III cycle is probably the initiation of a new upward transgression trend (Fig. 9).

Third and second order hemicycles

The Lagoa do Jacaré Formation in the Ubaí area has a clear general transgressive trend. Thick intervals of supra to intertidal zones at the base progressively shorten towards the top as the subtidal zones thicken. From the base to the top, microbial laminites and subaerial exposure surfaces are superseded by a higher amount of conglomeratic carbonates and packstones. This general transgressive trend is also supported by two outcrops above the studied interval and close to the 620 meters high that denote sedimentation in deeper water (upper shoreface; Fig. 11) than the peritidal carbonates. The higher-order transgression can be further subdivided into two lower order hemicycles, with a maximum regressive surface positioned, where microbial laminites become more frequent (top of the fifth-order c.3 and fourth-order c.I cycles). Thus, the general transgressive trend is interpreted as a second-order hemicycle subdivided into third-order regressive and transgressive hemicycles.

Paleoenvironmental evolution

From the analysis of the different cycle orders, it is conceived that the Lagoa do Jacaré Formation in the Ubaí area was a mud flat with spread microbial mats interbedded by tidal channel and sand carbonates deposits. The record suggests a dynamic coastal environment in terms of shoreline shifts and sea level fluctuations. The predominance of delicate microbial laminite, mudstone, and the low number of beds reworked by currents or waves, suggest peritidal carbonates from a low-angle ramp likely protected by oolitic shoals and microbial reefs. Thus, the lithofacies associations may be efficient paleobathymetric indicators (Masse *et al.* 2003). In general, as seen in the second-order hemicycle, the entire studied section was deposited during a sea level rise. Acording to Uhlein *et al.* (2019), in the Januária area, located 100 Km NE from the studied area, the Lagoa do Jacaré Formation initially yields a progradation and then a retrogradation of facies. The apex of regression is in the middle Lagoa do Jacaré Formation, which is marked by the first appearance of microbialite beds and tidal-related structures before the deepening of the basin (Uhlein *et al.* 2019). Other studied sections, such as the KM7-14 of Cui *et al.* (2020) or the Bom Despacho section from Santos *et al.* (2018) present low resolution stratigraphic data in a basin scale, and both are located in the southern basin approximately 600 km far south from Ubaí area. Therefore, we are able to tentatively correlate the Ubaí section with the beginning of the retrogradation tendency described by Uhlein *et al.* (2019) on the Januária paleo-high. In light of this, the Ubaí carbonates likely occur in the middle portion of the Lagoa do Jacaré Formation and record the beginning of the sea level rise that culminates in the deposition of shales from the Serra da Saudade Formation.

Internally to its regional transgression, the third-order shifts of the shoreline were seaward and then landward. These are responses to the fourth-order change, which in turn is composed of elemental fifth-order tidal cycles variation (Fig. 12). A direct correlation is made between the tidal cycle's thicknesses and shoreline shifts. The shortening or lengthening of the fifth-order cycles towards the top are related to a seaward or landward shoreline shift, respectively. Therefore, during the c.1 to c.3 cycles, the shoreline migrates seawards, and the tidal current has lower energy. Therefore, we observe a rise in organic and mud facies in the carbonate record. On the other hand, in c.4 and c.5 the shoreline migrates toward the continent, and the allochem-rich facies becomes frequent. Similar behavior happens in c.6 that migrates seaward, and with c.7 that migrates toward land (Fig. 12).

Figure 11. Grainstones that occur above the 620-meter height. On the left, in red, the hummocky stratification is highlighted. On the right, massive grainstones with weathering features.

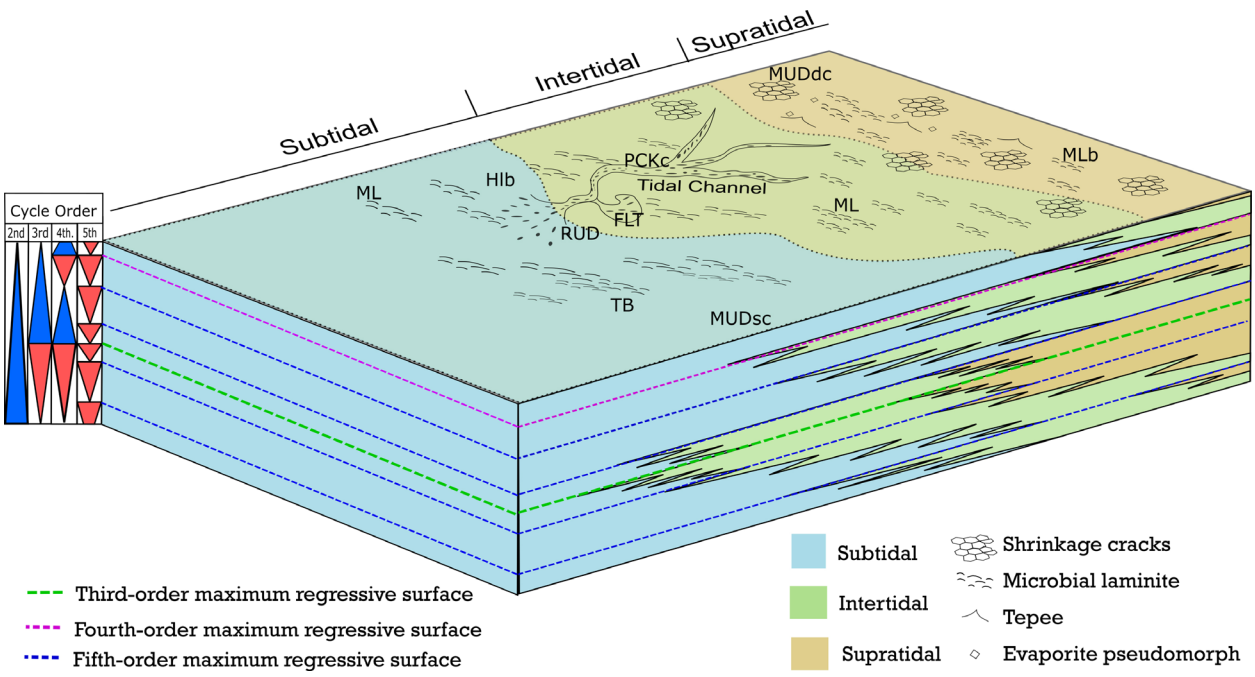

Figure 12. A schematic block diagram showing the paleoenvironmental evolution in a carbonate mud peritidal depositional system. Represented in this diagram are the progradations and retrogradations caused by the stratigraphic cycles and the distribution of the main lithofacies.

Tidal records in a restricted sea: how to reconcile?

The tidal cycles described in the Lagoa do Jacaré Formation in the Ubaí area bring the opportunity to discuss former interpretations of a restricted basin setting during much of the Bambuí Group deposition (e.g., Martins and Lemos 2007, Martins-Neto 2009, Uhlein *et al.* 2019, Cui *et al.* 2020, Caetano-Filho *et al.* 2021). Modern analogs of hundreds of thousands of square km enclosed seas, such as the Baltic, Caspian, and Black Sea, present strikingly small tidal ranges of less than 23 cm high (Levyant *et al.* 1994, Kulikov and Medvedev 2013, Medvedev *et al.* 2016). Although comprising huge areas on continents, these epicontinental seas have much smaller water masses than oceans and thus the effects of gravitational forces between Earth, Moon, and Sun are almost inexpressive. Stratigraphic analysis of ancient restricted basins suggests microtidal influence that in some cases are considered virtually non-tidal (Tucker and Wright 1990, Pratt 2010, James and Jones 2016). The thicknesses of each tide cycle here described are from 4 to 8 meters high (average = 6.4 m, n = 5). Thus, the tidal range recorded in the Lagoa do Jacaré carbonates in the Ubaí area is dozens of times higher than major modern enclosed seas. It is known that Precambrian oceans were likely subjected to stronger tidal forces due to a shorter distance between the Earth and the Moon (Williams 2000, Coughenour *et al.* 2009). Based on different possible Lunar recession rates, by the late Ediacaran, the Earth-Moon distance was the equivalent of 56 to 59 Earth radii (Williams 1994, 2000, Rodrigues *et al.* 2019). Once the current distance is approximately 60 Earth radii, the minimum and maximum ratios of the past to the present Earth-Moon distance ranges from 0.933 to 0.983 (6.7 to 1.7% difference) during the late Ediacaran, which gives increments of 1.04 to 1.16 times the modern gravitational force responsible for Earth tides. By these simple calculations, it is clear that an increase in the tidal forces due to a greater proximity between Earth and Moon is insufficient to explain macrotides in the late Ediacaran restricted basins.

Uhlein *et al.* (2019) showed a consistent trend of decreasing $\delta^{13}C$ values towards the top, from +15 to +6‰, in the 120 m-thick carbonates of the Lagoa do Jacaré Formation on the Januária paleo- high. Such a continuous isotopic shift is presumably linked to a progressive change in the basin's geographic and/or biochemical scenario towards more open ocean conditions (Cui *et al.* 2020). After a long period of basin restriction initiated at the upper Sete Lagoas Formation (Paula-Santos *et al.* 2017), our data suggest that the timing of a likely reopening of the Bambuí basin most likely occurred in the upper half of the Lagoa do Jacaré Formation. This hypothesis is based on isotopic data from the lower Serra da Saudade Formation, yielding lower $\delta^{13}C_{carb}$, $\delta^{13}C_{org}$, $\delta^{34}S_{pyrite}$ and higher $^{87}Sr/^{86}Sr$ signals compared with the lower half of the Lagoa do Jacaré Formation (Cui *et al.* 2020). Our novel sedimentologic and stratigraphic data reinforce these notions by suggesting a likely low-angle carbonate shelf developed on a semi-enclosed epicontinental sea, where due to funneling of the water flow, strong tidal currents and high tidal ranges act at the shore. The recovery from a restricted and highly methanogenic basin to a likely more open and oxidant sea water (see the youngest Bambuí carbonates in Uhlein *et al.* 2017, 2019, 2021) was likely slow and intermittent, with a duration of hundreds of thousands to a few million years.

CONCLUSIONS

Due to its particular geochemical dataset and recent interpretations of depositional settings and biogeochemical scenarios,

the Lagoa do Jacaré Formation is likely the most enigmatic stratigraphic unit of the basin. In this paper, we expanded the knowledge of the Lagoa do Jacaré formation by applying a high-resolution stratigraphic approach on 41 meters of microbialites and associated carbonatic rocks in Ubaí area, north of Minas Gerais. Sixteen lithofacies were grouped into subtidal, intertidal, and supratidal depozones of a peritidal environment and had their stratigraphic arrangement of second-order to fifth-order cycles unveiled and interpreted in terms of short and long-term sea level fluctuations. Seven asymmetrical tidal cycles (fifth-order cycles) with an average thickness of 6.4 meters were deposited during a regional transgression (second-order cycle). A correlation between tidal cycle thicknesses and tidal ranges on an ancient basin shore is feasible. Thus, the upper Lagoa do Jacaré Formation in Ubaí area was likely deposited during a time of strong tidal currents acting on the shore, which is only possible if the Bambuí basin was at least partially connected to the global ocean. We interpret a semi-enclosed epicontinental sea for part of the upper Lagoa do Jacaré Formation and suggest that a partial reopening of the Bambuí basin may have started in the upper Lagoa do Jacaré Formation. Our data reinforce the need for high-resolution sedimentologic and stratigraphic field data in order to properly understand the unique nature of the middle Bambuí units and the geotectonic framework of the basin during late Ediacaran and early Cambrian.

ARTICLE INFORMATION

Manuscript ID: 20210040. Received on: 29 MAY 2021. Approved on: 29 NOV 2021.

How to cite this article: Moura S.A., Uhlein A., Uhlein G.J., Dantas M.V.S. High-resolution stratigraphy of peritidal microbial carbonates from the Lagoa do Jacaré Formation, Bambuí Group, north of Minas Gerais state, Brazil. *Brazilian Journal of Geology*, 52(2):e20210040, 2022. https://doi.org/10.1590/2317-4889202120210040.

A.U. improved the manuscript through corrections and suggestions in all content; G.U. improved the manuscript through corrections and suggestions in all content; M.D. improved the manuscript through corrections and suggestions in the Discussion section.

Competing interests: The authors declare no competing interests.

REFERENCES

Alkmim F.F., Martins-Neto M.A. 2001. A bacia intracratônica do São Francisco: arcabouço estrutural e cenários evolutivos. *In*: Pinto C.P., Martins-Neto M.A. (Eds.). *Bacia do São Francisco:* geologia e recursos naturais. Belo Horizonte: Sociedade Brasileira de Geologia (SBG) e Núcleo MG, p. 9-30.

Atman D. 2011. *Controle lito-estrutural e estratigráfico na hidrogeoquímica e nas concentrações de fluoreto no Sistema aquífero cárstico-fissural do Grupo Bambuí, norte de Minas Gerais*. Thesis, Programa de Pós-Graduação em Geologia, Universidade Federal de Minas Gerais, Belo Horizonte, 131 p.

Awramik S.M. 1971. Precambrian columnar stromatolite diversity: reflection of metazoan appearance. *Science*, **174**(4011):825-827. https://doi.org/10.1126/science.174.4011.825

Bosak T., Knoll A.H., Petroff A.P. 2013. The meaning of stromatolites. *Annual Review of Earth and Planetary Sciences*, **41**:21-44. https://doi.org/10.1146/annurev-earth-042711-105327

Bosence D.W.J., Wood J.L., Rose E.P.F., Qing H. 2000. Low-and high-frequency sea-level changes control peritidal carbonate cycles, facies and dolomitization in the Rock of Gibraltar (Early Jurassic, Iberian Peninsula). *Journal of the Geological Society*, **157**:61-74. https://doi.org/10.1144/jgs.157.1.61

Burne R.V., Moore L.S. 1987. Microbialites; organosedimentary deposits of benthic microbial communities. *Palaios*, **2**(3):241-254. https://doi.org/10.2307/3514674

Caetano-Filho S., Sansjofre P., Ader M., Paula-Santos G., Guacaneme C., Babinski M., Bedoya-Rueda C., Kuchenbecker M., Reis H.L.S., Trindade R.I.F. 2021. A large epeiric methanogenic Bambuí sea in the core of Gondwana supercontinent? *Geoscience Frontiers*, **12**(1):203-218. https://doi.org/10.1016/j.gsf.2020.04.005

Caird R.A., Pufahl P.K., Hiatt E.E., Abram M.B., Rocha A.J.D., Kyser T.K. 2017. Ediacaran stromatolites and intertidal phosphorite of the Salitre Formation, Brazil: Phosphogenesis during the Neoproterozoic Oxygenation Event. *Sedimentary Geology*, **350**:55-71. https://doi.org/10.1016/j.sedgeo.2017.01.005

Canfield D.E., Poulton S.W., Narbonne G.M. 2007. Late-Neoproterozoic deep-ocean oxygenation and the rise of animal life. *Science*, **315**(5808):92-95. https://doi.org/10.1126/science.1135013

Castro P.T.A., Dardenne M.A. 2000. The sedimentology, stratigraphy and tectonic context of the São Francisco Supergroup at the southern boundary of the São Francisco craton, Brazil. *Revista Brasileira de Geociências*, **30**(3):345-437.

Catuneanu O. 2019. Model-independent sequence stratigraphy. *Earth-Science Reviews*, **188**:312-388. https://doi.org/10.1016/j.earscirev.2018.09.017

Caxito F.A., Halverson G.P., Uhlein A., Stevenson R., Dias T.G., Uhlein G.J. 2012. Marinoan glaciation in east central Brazil. *Precambrian Research*, **200-203**:38-58. https://doi.org/10.1016/j.precamres.2012.01.005

Caxito F.A., Lana C., Frei R., Uhlein G.J., Sial A.N., Dantas E.L., Pinto A.G., Campos F.C., Galvão P., Warren L.V., Okubo J., Ganade C.E. 2021. Goldilocks at the dawn of complex life: mountains might have damaged Ediacaran–Cambrian ecosystems and prompted an early Cambrian greenhouse world. *Scientific Reports*, **11**:20010. https://doi.org/10.1038/s41598-021-99526-z

Coughenour C.L., Archer A.W., Lacovara K.J. 2009. Tides, tidalites, and secular changes in the Earth–Moon system. *Earth-Science Reviews*, **97**(1-4):59-79. https://doi.org/10.1016/j.earscirev.2009.09.002

Cui H., Warren L.V., Uhlein G.J., Okubo J., Liu X.M., Plummer R.E., Baele S., Goderis P., Claeys P., Li F. 2020. Global or regional? Constraining the origins of the middle Bambuí carbon cycle anomaly in Brazil. *Precambrian Research*, **348**:105861. https://doi.org/10.1016/j.precamres.2020.105861

Dardenne M.A. 1978. Síntese sobre a estratigrafia do Grupo Bambuí no Brasil Central. *In*: Congresso Brasileiro de Geologia, **30**(2). *Anais*... SBG, p. 597-610.

Demicco R.V., Hardie L.A. 1994. *Sedimentary structures and early diagenetic features of shallow marine carbonate deposits (No. 1)*. SEPM Society for Sedimentary.

Drummond J.B.R., Pufahl P.K., Porto C.G., Carvalho M. 2015. Neoproterozoic peritidal phosphorite from the Sete Lagoas Formation,

Brazil, and the Precambrian P-cycle. *Sedimentology*, **62**(7):1978-2008. https://doi.org/10.1111/sed.12214

Dunham R.J. 1962. Classification of carbonate rocks according to depositional texture. *In*: Ham W.E. (Ed.). *Classification of carbonate rocks*. Tulsa: American Association of Petroleum Geologists, Memoir 1, p. 108-122.

Dupraz C., Reid R.P., Braissant O., Decho A.W., Norman R.S., Visscher P.T. 2009. Processes of carbonate precipitation in modern microbial mats. *Earth-Science Reviews*, **96**(3):141-162. https://doi.org/10.1016/j.earscirev.2008.10.005

Embry A.F. 1993. Transgressive–regressive (T–R) sequence analysis of the Jurassic succession of the Sverdrup Basin, Canadian Arctic Archipelago. *Canadian Journal of Earth Sciences*, **30**(2):301-320. https://doi.org/10.1139/e93-024

Embry A.F. 1995. Sequence boundaries and sequence hierarchies: problems and proposals. *In*: Steel, R.J., Felt, V.L., Johannessen, E.P., Mathieu, C. (eds.), Sequencestratigraphy on the Northwest European Margin. Norwegian Petroleum Society, **5**, 1-11.

Embry A.F., Klovan J.E. 1971. A Late Devonian Reef Tract on Northeastern Banks Island, Northwest Territories. *Bulletin of Canadian Petroleum Geology*, **19**(4):730-781. https://doi.org/10.35767/gscpgbull.19.4.730

Erwin D.H., Laflamme M., Tweedt S.M., Sperling E.A., Pisani D., Peterson K.J. 2011. The Cambrian conundrum: early divergence and later ecological success in the early history of animals. *Science*, **334**(6059):1091-1097. https://doi.org/10.1126/science.1206375

Fairchild T.R., Sanchez E.A.M. 2015. Microbialitos no Brasil: panorâmica de ocorrências e guia de caracterização morfológica. In: Fairchild T.R., Rohr R., Dias-Brito D. (eds.), *Microbialitos do Brasil do Pré-Cambiano ao recente:* um atlas. Rio de Janeiro: UNESPetro, 2015. v. 1, p. 10-20.

Folk, R.L. 1962. Spectral subdivision of limestone types. *In*: Ham, W.E. (Ed.). *Classification of carbonate rocks*. Tulsa: American Association of Petroleum Geolgists, I, p. 62-84.

Fragoso D.G.C., Uhlein A., Sanglard J.C.D., Suckau G.L., Guerzoni H.T.G., Faria P.H. 2011. Geologia dos grupos Bambuí, Areado e Mata da Corda na folha Presidente Olegário (1:100.000), MG: registro deposicional do Neoproterozóico ao Neocretáceo da Bacia do São Francisco. *Geonomos*, **19**(1):28-38. https://doi.org/10.18285/geonomos.v19i1.60

Freitas A.R., Uhlein A., Dantas M.V.S., Mendonça T.K. 2021. Caracterização em multiescala de carbonatos neoproterozóicos da Pedreira GMD, Formação Lagoa do Jacaré, Grupo Bambuí, Paraopeba-MG. *Geologia USP. Série Científica*, **21**(1):10-120. https://doi.org/10.11606/issn.2316-9095.v21-163573

Gaucher C., Sial A.N., Halverson G.P., Frimmel H.E. 2009. The Neoproterozoic and Cambrian: a time of upheavals, extremes and innovations. *In*: Gaucher C., Sial A.N., Halverson G.P., Frimmel H.E. (Eds.). Neoproterozoic-Cambrian tectonics, global changes and evolution: a focus on Southwestern Gondwan. *Developments in Precambrian Geology*, **16**:3-11.

Goldhammer, R.K., Dunn, P.A., Hardie, L.A. 1990. Depositional cycles, composite sea level changes, cycle stacking patterns, and the hierarchy of stratigraphic forcing--examples from platform carbonates of the Alpine Triassic. *Geological Society of America Bulletin*, **102**:535-562.

Haas J., Lobitzer H., Monostori M. 2007. Characteristics of the Lofer cyclicity in the type locality of the Dachstein Limestone (Dachstein Plateau, Austria). *Facies*, **53**(1):113-126. https://doi.org/10.1007/s10347-006-0087-8

Heineck, C.A., Leite, C.A.S., Silva, M.A., Vieira, V.S. 2003. *Mapa geológico do Estado de Minas Gerais, Escala 1:1.000.000*. Belo Horizonte: COMIG-CPRM.

Hercos C.M., Martins-Neto M.A., Danderfer F.A. 2008. Arcabouço estrutural da Bacia do São Francisco nos arredores da Serra da Água Fria (MG), a partir da integração de dados de superfície e sub-superfície. *Revista Brasileira de Geociências*, **38**(2-Supl. 1):197-212.

Hersi O.S., Dix G.R. 1999. Blackriveran (lower Mohawkian, Upper Ordovician) lithostratigraphy, rhythmicity, and paleogeography: Ottawa Embayment, eastern Ontario, Canada. *Canadian Journal of Earth Sciences*, **36**(12):2033-2050. https://doi.org/10.1139/e99-087

Iglesias M., Uhlein A. 2009. Estratigrafia do Grupo Bambuí e coberturas fanerozóicas no vale do rio São Francisco, norte de Minas Gerais. *Revista Brasileira de Geociências*, **39**(2):256-266.

Jahnert R.J., Collins L.B. 2011. Significance of subtidal microbial deposits in Shark Bay, Australia. *Marine Geology*, **286**(1-4):106-111. https://doi.org/10.1016/j.margeo.2011.05.006

James N.P. 1984. Shallowing-upward sequences in carbonates. *In*: Walker R.G. (Ed.). Facies models. *Geoscience Canada*, p. 126-136.

James N.P., Jones B. 2016. Origin of carbonate sedimentary rocks. Chichester: John Wiley & Sons.

Jimenez de Cisneros C., Vera J.A. 1993. Milankovitch cyclicity in Purbeck peritidal limestones of the Prebetic (Berriasian, southern Spain). *Sedimentology*, **40**(3):513-537. https://doi.org/10.1111/j.1365-3091.1993.tb01348.x

Kaufman A.J., Sial A.N., Frimmel H.E., Misi A. 2009. Neoproterozoic to Cambrian palaeoclimatic events in southwestern Gondwana. *In*: Gaucher C., Sial A.N., Halverson G.P., Frimmel H.E. (Eds.). Neoproterozoic-Cambrian tectonics, global change and evolution: a focus on Southwestern Gondwana. *Developments in Precambrian Geology*, p. 369-388.

Konhauser K.O., Amskold L., Lalonde S.V., Posth N.R., Kappler A., Anbar A. 2007. Decoupling photochemical Fe (II) oxidation from shallow-water BIF deposition. *Earth and Planetary Science Letters*, **258**(1-2):87-100. https://doi.org/10.1016/j.epsl.2007.03.026

Kuchenbecker M., Pedrosa-Soares A.C. 2010. O Grupo Bambuí na folha Luz (SE-23-Y-D-V). *Geonomos*, **18**(2):46-52. https://doi.org/10.18285/geonomos.v18i2.71

Kulikov E.A., Medvedev I.P. 2013. Variability of the Baltic Sea level and floods in the Gulf of Finland. *Oceanology*, **53**(2):145-151. https://doi.org/10.1134/S0001437013020094

Levyant A.S., Rabinovich B.I., Rabinovich A.B. 1994. Computation of seiche oscillations in seas of arbitrary configuration (exemplified by the Caspian Sea). *Oceanology*, **33**:588-598.

Li F., Deng J., Kershaw S., Burne R., Gong Q., Tang H., Lu C., Qu H, Zheng B., Luo S., Jin Z., Tan X. 2021. Microbialite development through the Ediacaran–Cambrian transition in China: distribution, characteristics, and paleoceanographic implications. *Global and Planetary Change*, **205**:103586. https://doi.org/10.1016/j.gloplacha.2021.103586

Logan B.W., Read J.F., Hagan G.M., Hoffman P., Brown R.W., Woods P.J., Gebelein C. 1974. Evolution and diagenesis of Quaternary carbonate sequences, Shark Bay, Western Australia. Memoirs – American Association of Petroleum Geologists, **22**:140-194. https://doi.org/10.1306/M22379

Magalhães P.M. 1989. *Análise estrutural qualitativa das rochas do Grupo Bambuí, na porção sudoeste da Bacia do São Francisco*. Dissertation, DEGEO/Escola de Minas, Universidade Federal de Ouro Preto, Ouro Preto, 100 p.

Martins M., Lemos V.L. 2007. Análise estratigráfica das sequências neoproterozoicas da Bacia do São Francisco. *Revista Brasileira de Geociências*, **37**(4 Suppl.):156-167.

Martins-Neto M.A. 2009. Sequence stratigraphic framework of Proterozoic successions in eastern Brazil. *Marine and Petroleum Geology*, **26**(2):163-176. https://doi.org/10.1016/j.marpetgeo.2007.10.001

Martins-Neto M.A., Alkmim F.F. 2001. Estratigrafia e evolução tectônica das bacias neoproterozóicas do Paleocontinente São Francisco e suas margens: Registro da quebra de Rodínia e colagem de Gondwana. *In*: Pinto C.P., Martins-Neto M.A. (Eds.). *Bacia do São Francisco:* geologia e recursos naturais. Belo Horizonte: SBG/MG, p. 31-54.

Masse J.P., Fenerci M., Pernarcic E. 2003. Palaeobathymetric reconstruction of peritidal carbonates Late Barremian, Urgonian, sequences of Provence (SE France). *Palaeogeography, Palaeoclimatology, Palaeoecology*, **3132**:1-17.

Medvedev I.P., Rabinovich A.B., Kulikov E.A. 2016. Tides in three enclosed basins: the Baltic, Black, and Caspian seas. *Frontiers in Marine Science*, **3**:46. https://doi.org/10.3389/fmars.2016.00046

Meert J.G., Lieberman B.S. 2008. The Neoproterozoic assembly of Gondwana and its relationship to the Ediacaran–Cambrian radiation. *Gondwana Research*, **14**(1-2):5-21. https://doi.org/10.1016/j.gr.2007.06.007

Miall A.D. 1977. A review of the braided-river depositional environment. *Earth-Science Reviews*, **13**(1):1-62. https://doi.org/10.1016/0012-8252(77)90055-1

Misi A. 2001. Estratigrafia isotópica das seqüências do Supergrupo São Francisco, coberturas neoproterozóicas do Cráton do São Francisco. Idade e correlações. *Bacia do São Francisco*. Geologia e Recursos Naturais. SBG, Núcleo de Minas Gerais, p. 67-92.

Misi A., Kaufman A.J., Veizer J., Powis K., Azmy K., Boggiani P.C., Gaucher C., Teixeira J.B.G., Sanches A.L., Iyer S.S.S. 2007. Chemostratigraphic correlation of Neoproterozoic successions in South America. *Chemical Geology*, **237**:161-185. http://doi.org/10.1016/j.chemgeo.2006.06.019

Moreira D.S., Uhlein A., Dussin I.A., Uhlein G.J., Misuzaki A.M.P. 2020. A Cambrian age for the upper Bambuí Group, Brazil, supported by the first U-Pb dating of volcaniclastic bed. *Journal of South American Earth Sciences*, **99**:102503. https://doi.org/10.1016/j.jsames.2020.102503

Moynihan D.P., Strauss J.V., Nelson L.L., Padget C.D. 2019. Upper Windermere Supergroup and the transition from rifting to continent-margin sedimentation, Nadaleen River area, northern Canadian Cordillera. *Bulletin*, **131**(9-10):1673-1701. https://doi.org/10.1130/B32039.1

Myshrall K.L., Mobberley J.M., Green S.J., Visscher P.T., Havemann S.A., Reid R.P., Foster J.S. 2010. Biogeochemical cycling and microbial diversity in the thrombolitic microbialites of Highborne Cay, Bahamas. *Geobiology*, **8**(4):337-354. https://doi.org/10.1111/j.1472-4669.2010.00245.x

Na L., Kiessling W. 2015. Diversity partitioning during the Cambrian radiation. Proceedings of the National Academy of Sciences of the United States of America, **112**(15):4702-4706. https://doi.org/10.1073/pnas.1424985112

Och L.M., Shields-Zhou G. 2012. The Neoproterozoic oxygenation event: environmental perturbations and biogeochemical cycling. *Earth-Science Reviews*, **110**(1-4):26-57. https://doi.org/10.1016/j.earscirev.2011.09.004

Osleger D., Read J.F. 1991. Relation of eustasy to stacking patterns of meter-scale carbonate cycles, Late Cambrian, USA. *Journal of Sedimentary Research*, **61**(7):1225-1252. https://doi.org/10.1306/D426786B-2B26-11D7-8648000102C1865D

Paula-Santos G.M., Babinski M., Kuchenbecker M., Caetano-Filho S., Trindade R.I., Pedrosa-Soares A.C. 2015. New evidence of an Ediacaran age for the Bambuí Group in Southern São Francisco craton (eastern Brazil) from zircon U–Pb data and isotope chemostratigraphy. *Gondwana Research*, **28**(2):702-720. https://doi.org/10.1016/j.gr.2014.07.012

Paula-Santos G.M., Caetano-Filho S., Babinski M., Trindade R.I.F., Guacaneme C. 2017. Tracking connection and restriction of West Gondwana São Francisco basin through isotope chemostratigraphy. *Gondwana Research*, **42**:280-305. https://doi.org/10.1016/j.gr.2016.10.012

Peterhänsel A.R.N.D.T., Egenhoff S.O. 2008. Lateral variabilities of cycle stacking patterns in the Latemar, Triassic, Italian Dolomites. *SEPM Special Publication*, **89**:217-229. https://doi.org/10.2110/pec.08.89.0217

Pimentel M.M., Rodrigues J.B., DellaGiustina M.E.S., Junges S., Matteini M., Armstrong R. 2011. The tectonic Evolution of the Neoproterozoic Brasília Belt, central Brazil, based on SHRIMP and LA-ICPMS U–Pb sedimentary provenance data: a review. *Journal of South American Earth Sciences*, **31**(4):345-357. https://doi.org/10.1016/j.jsames.2011.02.011

Pratt B.R. 2010. Peritidal carbonates. *In*: James N.P., Dalrymple R.W. (Eds.). *Facies Models 4*. Geological Association of Canada, p. 401-420.

Quijada I.E., Benito M.I., Suarez-Gonzalez P., Rodríguez-Martínez M., Campos-Soto S. 2020. Challenges to carbonate-evaporite peritidal facies models and cycles: Insights from Lower Cretaceous stromatolite-bearing deposits (Oncala Group, N Spain). *Sedimentary Geology*, **408**:105752. https://doi.org/10.1016/j.sedgeo.2020.105752

Read J.F., Goldhammer R.K. (1988). Use of Fischer plots to define third-order sea-level curves in Ordovician peritidal cyclic carbonates, Appalachians. *Geology*, **16**(10):895-899. https://doi.org/10.1130/0091-7613(1988)016%3C0895:UOFPTD%3E2.3.CO;2

Reis H.L.S., Alkmim F.F., Fonseca R.C.S., Suss J.F., Nascimento T.C., Prrevatti L.D. 2016. The São Francisco Basin. *In*: Heilbron M., Cordani U.G., Alkmim F. (Eds.). *São Francisco Craton, Eastern Brazil:* tectonic genealogy of a miniature continent. Switzerland: Springer, p. 117-143.

Reis H.L.S., Suss J.F., Fonseca R.C.S., Alkmim F.F. 2017. Ediacaran forebulge grabens of the southern São Francisco basin, SE Brazil: craton interior dynamics during West Gondwana assembly. *Precambrian Research*, **302**:150-170. https://doi.org/10.1016/j.precamres.2017.09.023

Ribeiro A., Paciulo F.V.P., Senra A.S., Valeriano C.M., Trouw R.A.J. 2008. *Geologia da Folha de Piumhi SF.23-V-B-2*. Programa Geologia do Brasil. Rio de Janeiro: CPRM-UFRJ.

Riding R. 2000. Microbial carbonates: the geological record of calcified bacterial–algal mats and biofilms. *Sedimentology*, **47**(Suppl. 1):179-214. https://doi.org/10.1046/j.1365-3091.2000.00003.x

Riding R. 2006. Cyanobacterial calcification, carbon dioxide concentrating mechanisms, and Proterozoic–Cambrian changes in atmospheric composition. *Geobiology*, **4**(4):299-316. https://doi.org/10.1111/j.1472-4669.2006.00087.x

Riding R. 2011. Microbialites, stromatolites, and thrombolites. *In*: Reitner J., Thiel V. (Eds.). *Encyclopedia of geobiology*. Switzerland: Springer, p. 635-654.

Rodrigues P.D.O.C., Hinnov L.A., Franco D.R. 2019. A new appraisal of depositional cyclicity in the Neoarchean-Paleoproterozoic Dales Gorge Member (Brockman Iron Formation, Hamersley Basin, Australia). *Precambrian Research*, **328**:27-47. https://doi.org/10.1016/j.precamres.2019.04.007

Sanchez E.A., Uhlein A., Fairchild T.R. 2021. Treptichnus pedum in the Tres Marias Formation, south-central Brazil, and its implications for the Ediacaran-Cambrian transition in South America. *Journal of South American Earth Sciences*, **105**:102983. https://doi.org/10.1016/j.jsames.2020.102983

Santos D.M., Sanchez E.A., Santucci R.M. 2018. Morphological and petrographic analysis of identified stromatolitic occurrences in Lagoa do Jacaré Formation, Bambuí Group, state of Minas Gerais, Brazil. A Journal of the *Brazilian Society of Paleontology*, **21**(3):195-207. https://doi.org/10.4072/rbp.2018.3.01

Schopf J.W., Kudryavtsev A.B., Czaja A.D., Tripathi A.B. 2007. Evidence of Archean life: stromatolites and microfossils. *Precambrian Research*, **158**(3-4):141-155. https://doi.org/10.1016/j.precamres.2007.04.009

Sial A.N., Dardenne M.A., Misi A., Pedreira A.J., Gaucher C., Ferreira V.P., Silva Filho M.A., Uhlein A., Pedrosa-Soares A.C., Santos R.V., Egydio-Silva M., Babinski M., Alvarenga C.J.S., Fairchild T.R., Pimentel M.M. 2009. The São Francisco Palaeocontinent. *In*: Gaucher C., Sial A.N., Halverson G.P., Frimmel H.E. (Eds). Neoproterozoic-Cambrian tectonics, global change and evolution: a focus on southwestern Gondwana. *Developments in Precambrian Geology*, **16**:31-69.

Signorelli N. 2009. *Folha SE. 23-Y-D-III Abaeté: Projeto Sete Lagoas - Abaeté*. Programa Geologia do Brasil. Belo Horizonte.

Spence G.H., Tucker M.E. 2007. A proposed integrated multi-signature model for peritidal cycles in carbonates. *Journal of Sedimentary Research*, **77**(10):797-808. https://doi.org/10.2110/jsr.2007.080

Tucker M.E. 2003. *Sedimentary rocks in the field*. Chichester: John Wiley & Sons.

Tucker M.E., Wright V.P. 1990. *Carbonate sedimentology*. Oxford: Blackwell Science, 482 p.

Uhlein A., Reis Junior W., Freitas A.R., Uhlein G.J, Ávila M.A.B. 2014. *Projeto Norte de Minas Folha Ubaí SE-23-X-A-I*. Escala 1:100.000. Minas Gerais: CODEMIG.

Uhlein G.J. 2017. *Análise de bacia sedimentar e quimioestratigrafia do Grupo Bambuí em Minas Gerais*. Thesis, Instituto de Geociências, Universidade Federal de Minas Gerais, Belo Horizonte, 125 p.

Uhlein G.J., Caxito F.A., Frei R., Uhlein A., Sial A.N., Dantas E.L. 2021. Microbially induced chromium isotope fractionation and trace elements behavior in lower Cambrian microbialites from the Jaíba Member, Bambuí Basin, Brazil. *Geobiology*, **19**(2):125-146. https://doi.org/10.1111/gbi.12426

Uhlein G.J., Uhlein A., Pereira E., Caxito F.A., Okubo J., Warren L., Sial A.N. 2019. Ediacaran paleoenvironmental changes recorded in the mixed carbonate-siliciclastic Bambuí Basin, Brazil. *Palaeogeography, Palaeoclimatology, Palaeoecology*, **517**:39-51. http://doi.org/10.1016/j.palaeo.2018.12.022

Uhlein G.J., Uhlein A., Stevenson R., Halverson G.P., Caxito F.A., Cox G.M. 2017. Early to late Ediacaran conglomeratic wedges from a complete foreland basin cycle in the southwest São Francisco Craton, Bambuí Group, Brazil. *Precambrian Research*, **299**:101-116. https://doi.org/10.1016/j.precamres.2017.07.020

Van Gemerden, H. 1993. Microbial Mats: a joint Venture. *Marine Geology*, **113**(1-2):3-25. https://doi.org/10.1016/0025-3227(93)90146-M

Vasconcelos C., Bahniuk A. 2015. Microbialitos recentes da região dos Lagos, Estado do Rio de Janeiro. *In*: Fairchild T.R., Rohn R., Dias-Brito D. (Eds.). *Microbialitos do Brasil:* do Pré-Cambriano ao Recente. São Paulo: IGCE/UNESP, p. 60-75.

Vasconcelos, C., Dittrich, M., McKenzie, J.A. 2014. Evidence of microbiocoenosis in the formation of laminae in modern stromatolites. *Facies*, **60**(1):3-13. https://doi.org/10.1007/s10347-013-0371-3

Visscher P.T., Stolz J.F. 2005. Microbial mats as bioreactors: populations, processes, and products. *Palaeogeography, Palaeoclimatology, Palaeoecology*, **219**(1-2):87-100. https://doi.org/10.1016/j.palaeo.2004.10.016

Warren L.V., Quaglio F., Riccomini C., Simões M.G., Poiré D.G., Strikis N.M., Anelli L.E., Strikis P.C. 2014. The puzzle assembled: Ediacaran guide fossil Cloudina reveals an old proto-Gondwana seaway. *Geology*, **42**(5):391-394. https://doi.org/10.1130/G35304.1

Williams G.E. 1994. History of Earth's rotation and the Moon's orbit: a key datum from Precambrian strata in Australia. *Australian Journal of Astronomy*, **5**(4):135-147.

Williams G.E. 2000. Geological constraints on the Precambrian history of Earth's rotation and the Moon's orbit. *Reviews of Geophysics*, **38**(1):37-59. https://doi.org/10.1029/1999RG900016

Wright V.P., Burchette T.P. 1996. Shallow-water carbonate environments. *In*: Reading H.G. (Ed.). *Sedimentary environments, facies and stratigraphy*. Oxford: Blackwell Science, p. 325-394.

Yanez-Montalvo A., Gómez-Acata S., Águila B., Hernández-Arana H., Falcón L.I. 2020. The microbiome of modern microbialites in Bacalar Lagoon, Mexico. *PLoS One*, **15**(3):e0230071. https://doi.org/10.1371%2Fjournal.pone.0230071

Yang W., Lehrmann D.J., Hu X.-F. 2014. Peritidal carbonate cycles induced by carbonate productivity variations: a conceptual model for an isolated Early Triassic greenhouse platform in South China. *Journal of Palaeogeography*, **3**(2):115-126. https://doi.org/10.3724/SP.J.1261.2014.00047

Zalán P.V., Romeiro-Silva P.C. 2007. Bacia do São Francisco. *Boletim de Geociências da Petrobras*, **15**(2):561-570.

Zhang Y., Chen D., Zhou X., Guo Z., Wei W., Mutti M. 2015. Depositional facies and stratal cyclicity of dolomites in the Lower Qiulitag Group (Upper Cambrian) in northwestern Tarim Basin, NW China. *Facies*, **61**(1):417. https://doi.org/10.1007/s10347-014-0417-1

Zhu M.Y., Zhuravlev A.Y., Wood R.A., Zhao F.C., Sukhov S.S. 2017. A deep root for the Cambrian explosion: Implications of new bio-and chemostratigraphy from the Siberian Platform. *Geology*, **45**(5):459-462. https://doi.org/10.1130/G38865.1